MEASUREMENT OF WASTEWATER ANALYTES USING HIGH-THROUGHPUT RAMAN SPECTROSCOPY

Michael Shea
40 Manning Road
Billerica, MA 01821

Shaun Fraser
40 Manning Road
Billerica, MA 01821

Nathan Simonds
40 Manning Road,
Billerica, MA 01821

KEYWORDS

Raman Spectroscopy, Process Monitoring, Wastewater, Oxyanions, Nitrogen Compounds, Residual Solvents, Quantification, Process Analyzer Technology, Laboratory Analysis

ABSTRACT

Industrial wastewater streams contain a diverse range of nitrogen-containing compounds, oxyanions, and residual solvents that must be monitored to meet regulatory requirements, reduce treatment costs, and enable material recovery. This work demonstrates the application of high-throughput Raman spectroscopy for the rapid, in situ measurement of key wastewater analytes. Using Bruker's High-Throughput Virtual Slit (HTVS™) Raman spectrometers, quantitative models were developed with minimal sample preparation and short acquisition times, typically 30 seconds per measurement. Multivariate analysis enabled accurate identification and quantification of multiple species in aqueous matrices, with limits of detection reaching the low-ppm range. Results highlight the ability of Raman

spectroscopy to distinguish closely related species and to simultaneously monitor multiple compounds under identical measurement conditions. These findings demonstrate that high-throughput Raman spectroscopy is a powerful tool for real-time wastewater monitoring, supporting process understanding, regulatory compliance, and cost-effective wastewater management across a wide range of industrial applications.

INTRODUCTION

Modern manufacturing processes generate increasingly diverse and concentrated contaminants, contributing to the growing complexity of industrial wastewater management. Contaminants vary by industry, but some common classes are oxyanions, nitrogen-containing species, and residual solvents (1). Beyond their environmental impact, these constituents can also present opportunities for resource recovery when effectively monitored and managed. At the same time, regulatory requirements (such as those established under the Clean Water Act in the United States and similar frameworks globally) set stringent discharge limits, creating a need for analytical approaches that are both accurate and efficient for comprehensive wastewater characterization (2).

Some traditional analytical techniques used for wastewater monitoring include ion chromatography, gas chromatography, and mass spectrometry. While they offer both high sensitivity and specificity, they are typically labor-intensive, requiring extensive sample preparation. Additionally, they are not easily transferred to real-time in situ measurements (3). This limits the ability to make rapid decisions and optimize processes. As a result, there is increasing interest in spectroscopic techniques that enable rapid, non-destructive, and multiplexed analysis of complex aqueous systems.

Raman spectroscopy offers molecular specificity and the capability to analyze samples without the need for extensive sample preparation (4). Unlike infrared spectroscopy, Raman spectroscopy is relatively insensitive to water, making it well-suited for aqueous matrices, like wastewater. In this context, the application of high-throughput Raman spectroscopy offers a compelling solution for real-time, in situ monitoring of industrial wastewater streams. Another key strength of Raman spectroscopy is its compatibility with process analytical technology frameworks. Fiber optic probes can be inserted into pipes, tanks, or reaction vessels. This allows for continuous, real-time monitoring.

By reducing analysis time, minimizing sample handling, and enabling multiplexed detection, Raman-based methods have the potential to improve regulatory compliance, reduce operational costs, and facilitate resource recovery. This work builds on these advances by demonstrating the effectiveness of high-throughput Raman spectroscopy for the rapid quantification of common wastewater analytes.

EXPERIMENTAL

All samples were prepared in a laboratory setting in separate solutions. The samples were measured using a HyperFlux PRO Plus with a Hudson Immersion Probe. Table I shows the measurement parameters used for each set of samples. The chemometric software, PEAXACT, was used to build partial least squares (PLS) models. For preprocessing, rubber band subtraction, 11-point smoothing, and peak normalization to the sapphire band (400-430cm^{-1}) were performed.

TABLE I. MEASUREMENT PARAMETERS.

COMPOUND	MEASUREMENT RANGE	MEASUREMENT ERROR (RMSECV)	TOTAL MEASUREMENT TIME
Phosphate	250-3000ppm	96ppm	30s
HPO4	250-1500ppm	203ppm	30s
H2PO4	250-1500ppm	95ppm	30s
H3PO4	250-3000ppm	50ppm	30s
Nitrate	13-140ppm	3.8ppm	30s
Nitrite	250-3000ppm	92ppm	30s
Sulfate	14-50ppm	2.4ppm	15s
Sulfite	250-3000ppm	72ppm	30s
Perchlorate	0.1-21ppm	0.84ppm	1.25min
Urea	250-3000ppm	20ppm	30s
Ammonium	0.1-5%	0.20%	30s
Dichloromethane	10-50ppm	17ppm	3min
Acetonitrile	0-1000ppm	3.6ppm	15min with OPIS and mux
			30s using SFx

Results and Discussion

PHOSPHATE RESULTS

Figure 1 shows the overlaid spectra of the phosphate species (H_3PO_4, $H_2PO_4^-$, HPO_4^{2-}, and PO_4^{3-}).

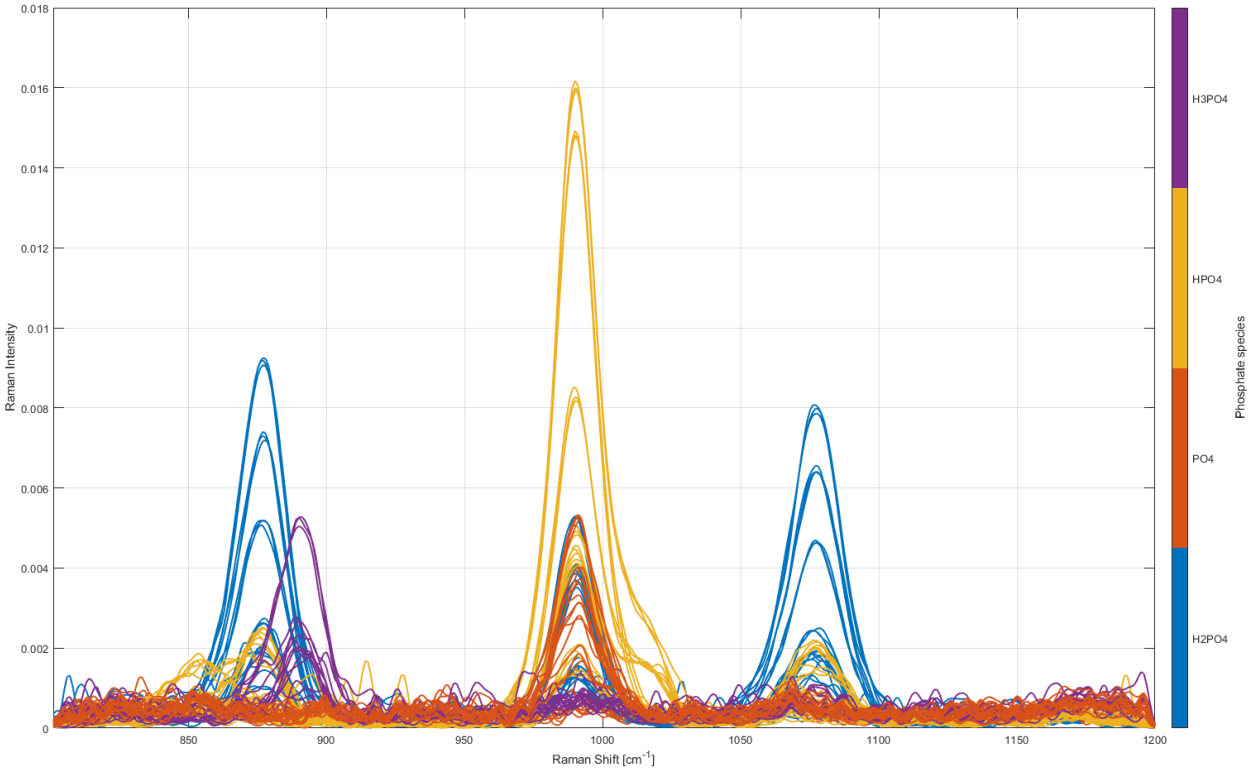

FIGURE 1. SPECTRA OF PHOSPHATE SPECIES.

A separate PLS model was made for each of the phosphate species studied (H_3PO_4, $H_2PO_4^-$, HPO_4^{2-}, and PO_4^{3-}) from their respective spectra. Each PLS model was one-factor. The predicted versus true and difference versus true plots corresponding to the PLS models for H_3PO_4 (Figure 2), $H_2PO_4^-$ (Figure 3), HPO_4^{2-} (Figure 4), and PO_4^{3-} (Figure 5) are shown.

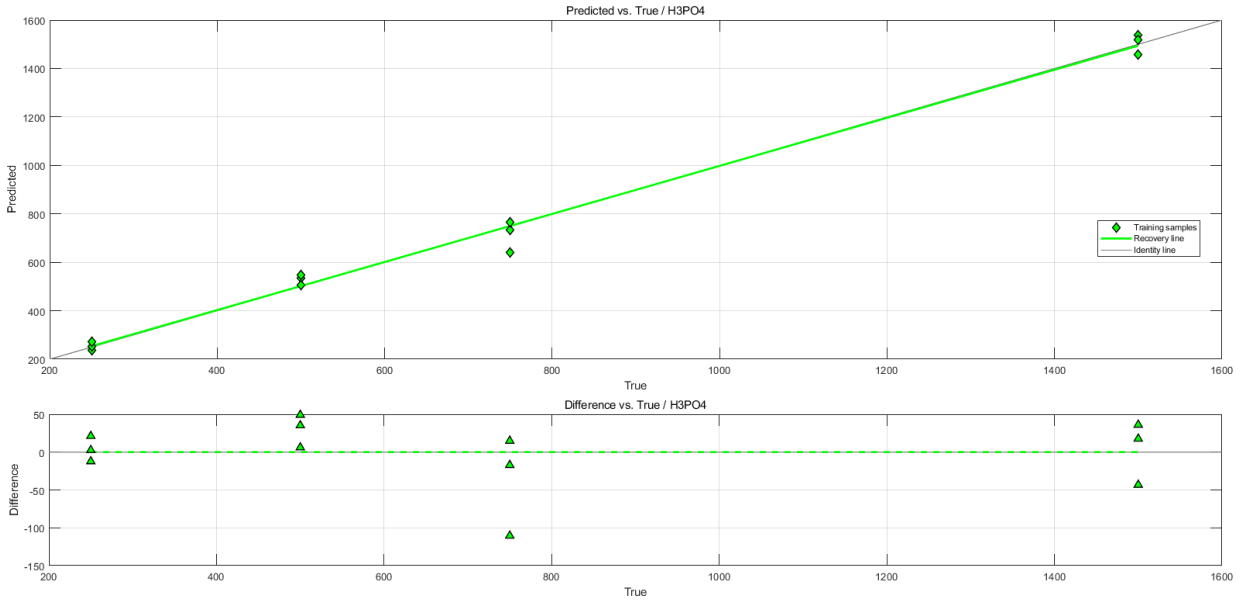

FIGURE 2. PREDICTED VS TRUE AND DIFFERENCE VS TRUE PLOTS FOR H_3PO_4.

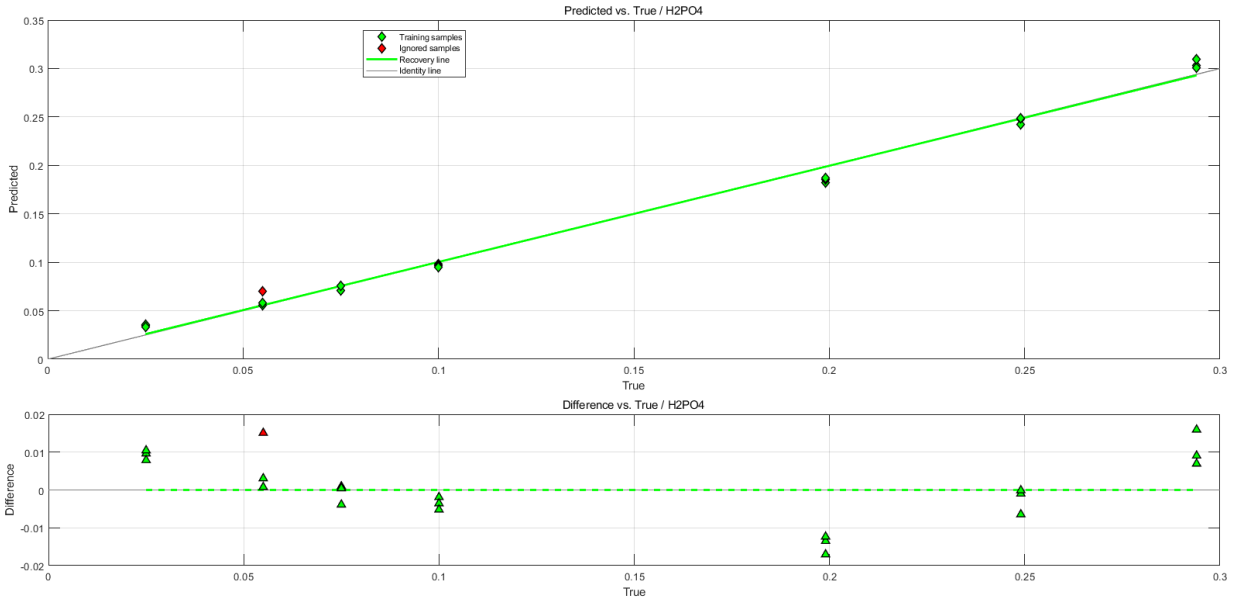

FIGURE 3. PREDICTED VS TRUE AND DIFFERENCE VS TRUE PLOTS FOR $H_2PO_4^-$.

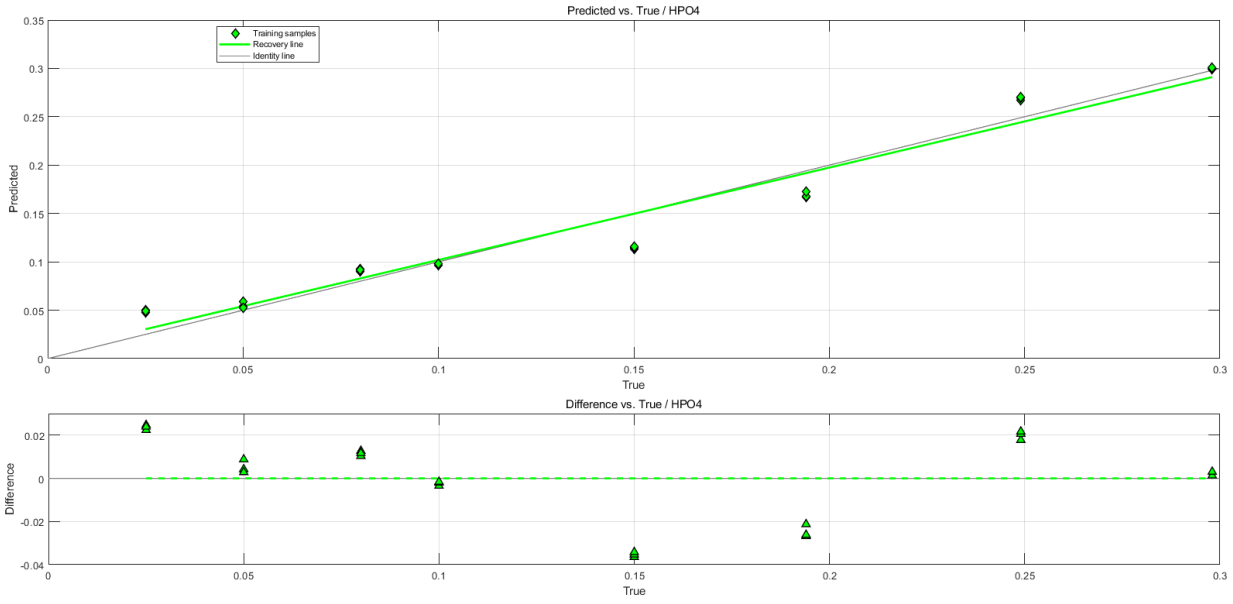

FIGURE 4. PREDICTED VS TRUE AND DIFFERENCE VS TRUE PLOTS FOR HPO_4^{2-}.

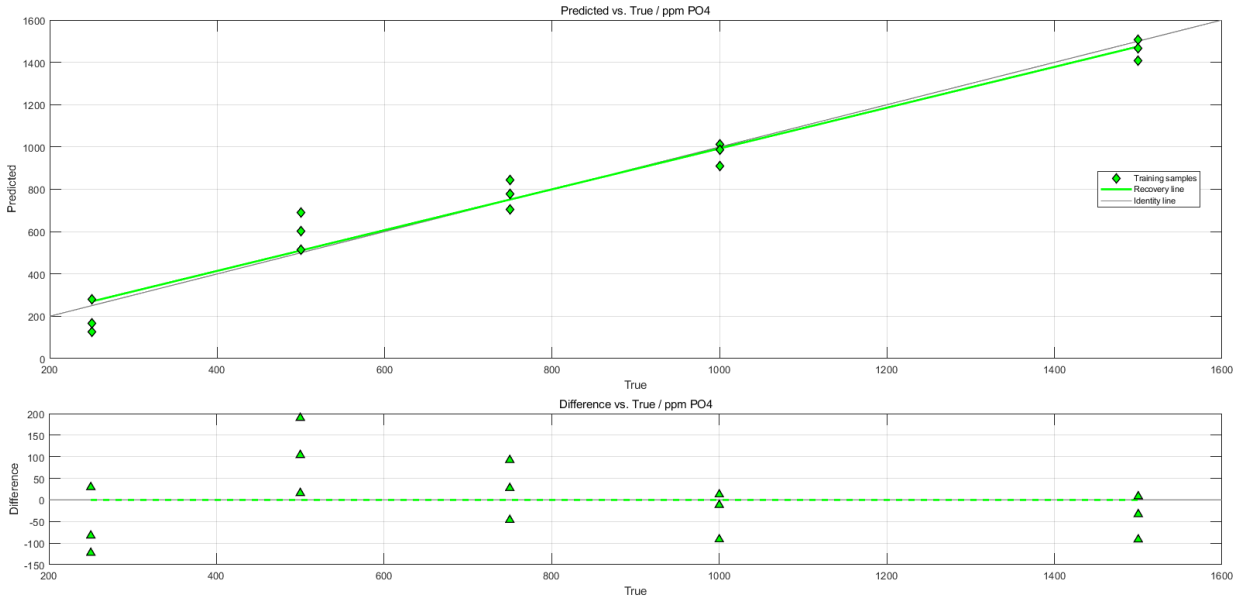

FIGURE 5. PREDICTED VS TRUE AND DIFFERENCE VS TRUE PLOTS FOR PO_4^{3-}.

PHOSPHATE DISCUSSION

The bands at 850-900cm^{-1} and 1050-1100cm^{-1} are associated with POH bonds. The band at 980-1020cm^{-1} is associated with PO bonds. The band associated with the POH bonds gave a stronger response than the band associated with the PO bonds. The multiple bands allow for the different degrees of protonation among the phosphates to be identified and they are distinct from other compounds.

NITRATE AND NITRITE RESULTS

Figures 6 and 7 show the spectra of nitrate and nitrite, respectively. Nitrate was measured over a range of 13ppm to 140ppm. Nitrite was measured over a range of 300ppm to 3000ppm.

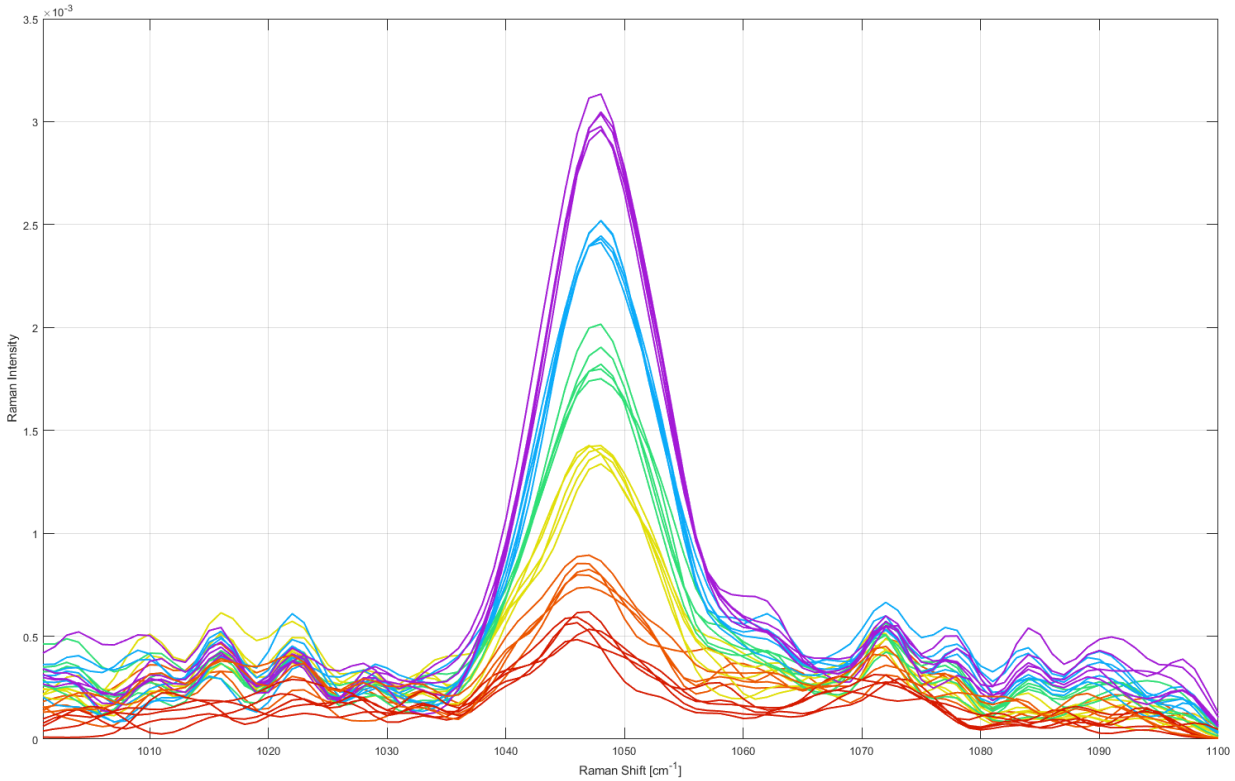

FIGURE 6. SPECTRA OF NITRATE SAMPLES FROM 13PPM TO 140PPM.

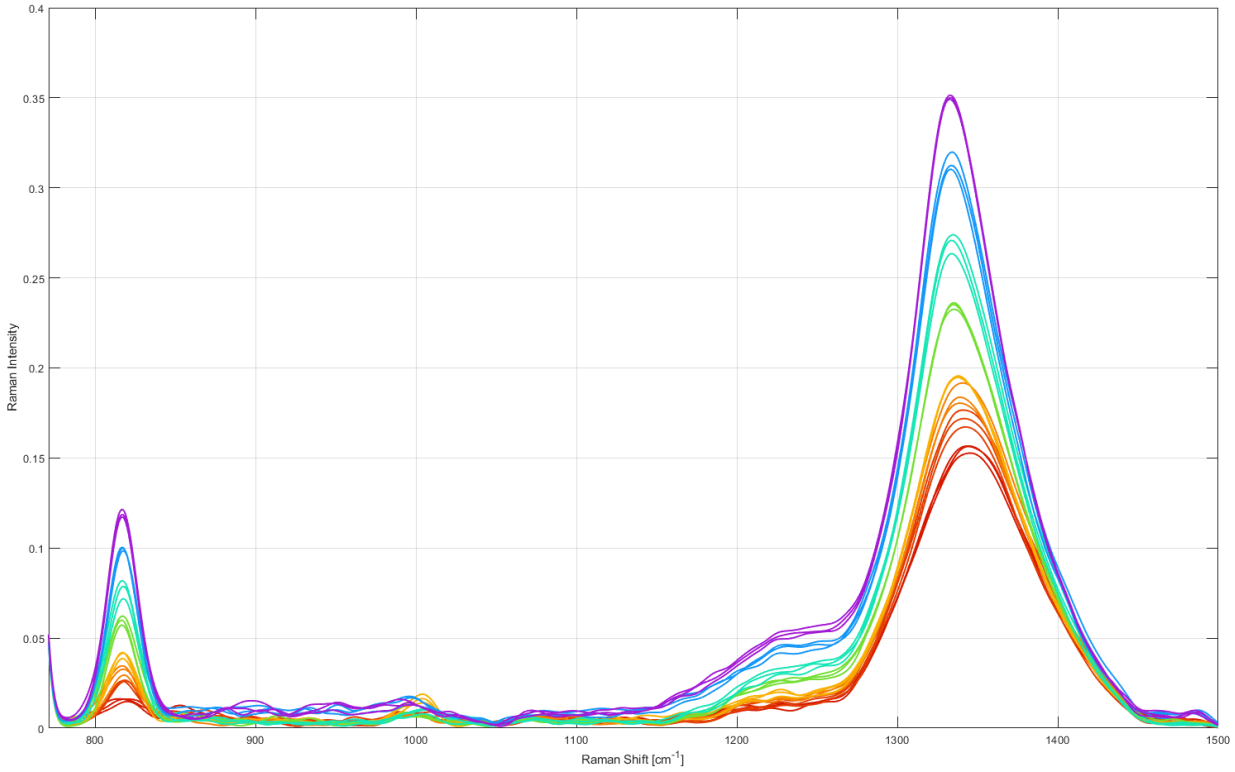

FIGURE 7. SPECTRA OF NITRATE SAMPLES FROM 300PPM TO 3000PPM.

A separate PLS model was made for both nitrate and nitrite from their respective spectra. Each PLS model was one-factor. The predicted versus true and difference versus true plots corresponding to the PLS models for nitrate (Figure 8) and nitrite (Figure 9) are shown.

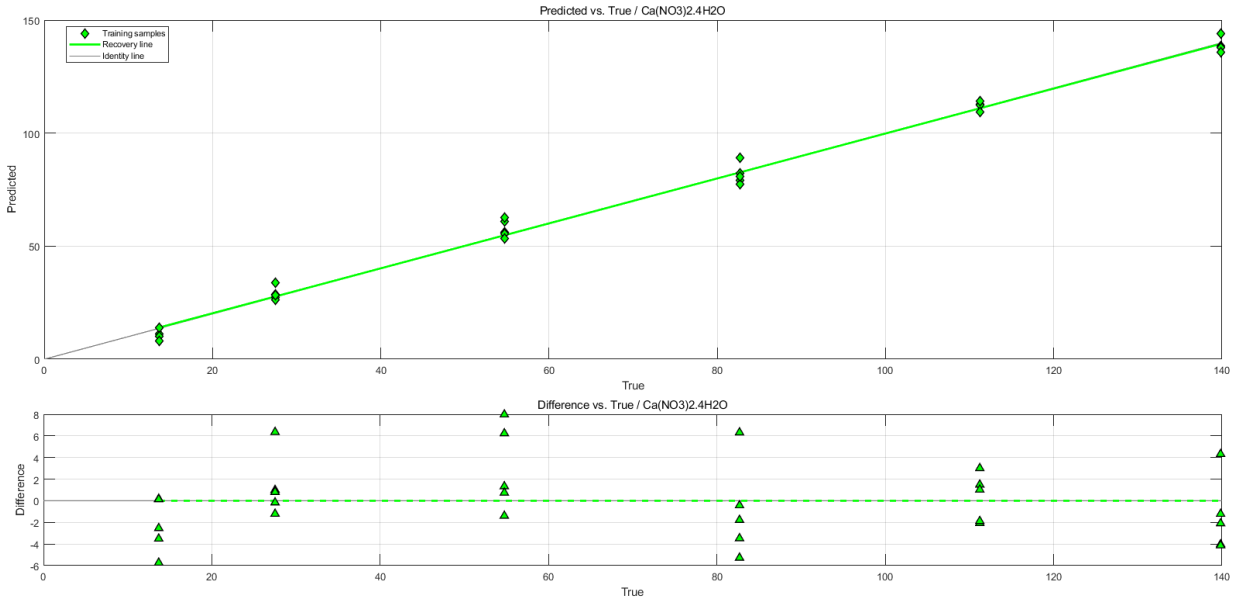

FIGURE 8. PREDICTED VS TRUE AND DIFFERENCE VS TRUE PLOTS FOR NITRATE.

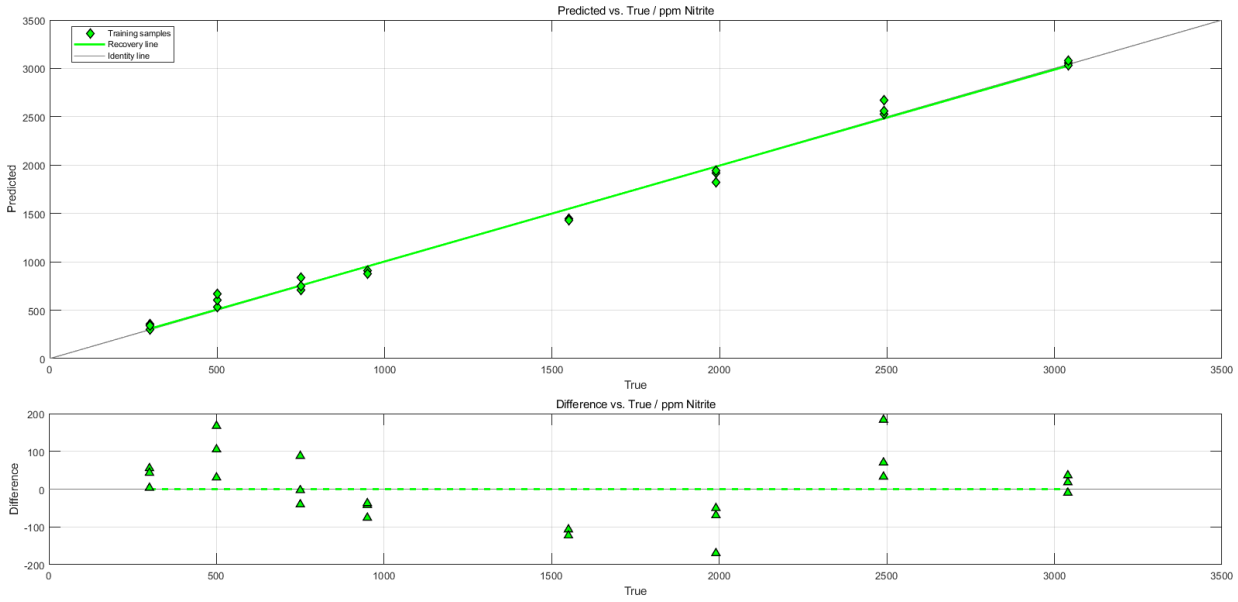

FIGURE 9. PREDICTED VS TRUE AND DIFFERENCE VS TRUE PLOTS FOR NITRITE.

NITRATE AND NITRITE DISCUSSION

The band shown in Figure 6 is distinct from the phosphate and nitrite bands. The band from 800-850cm^{-1} in Figure 7 is distinct from the other analytes.

SULFATE AND SULFITE RESULTS

Figures 10 and 11 show the spectra of sulfate and sulfite, respectively. Sulfate was measured over a range of 14ppm to 50ppm. Sulfite was measured over a range of 250ppm to 3000ppm.

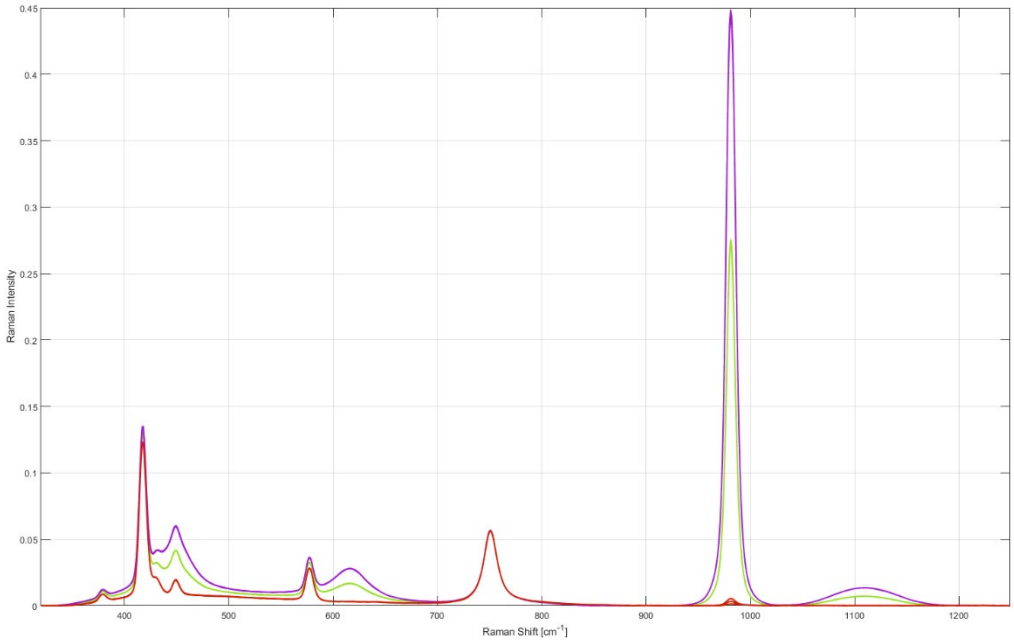

FIGURE 10. SPECTRA OF SULFATE SAMPLES FROM 14PPM TO 50PPM.

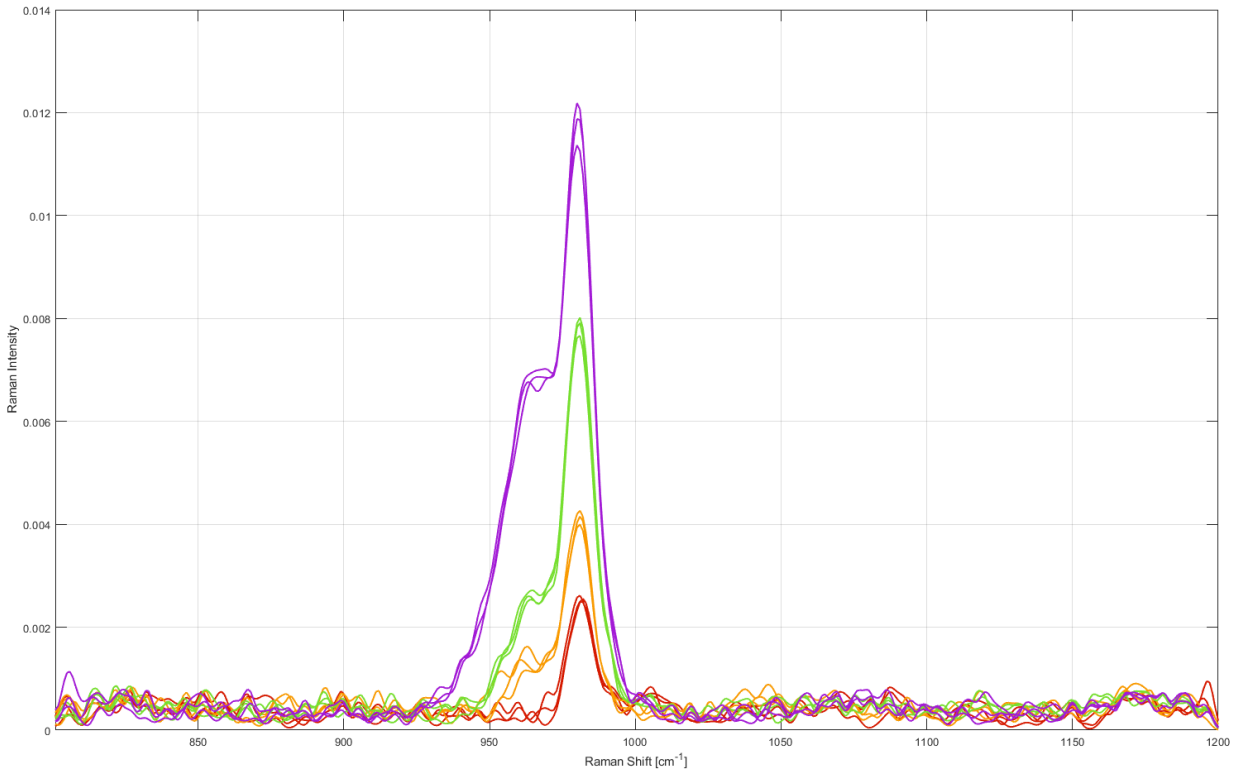

FIGURE 11. SPECTRA OF SULFITE SAMPLES FROM 250PPM TO 3000PPM.

A separate PLS model was made for both sulfate and sulfite from their respective spectra. Each PLS model was one-factor. The predicted versus true and difference versus true plots corresponding to the PLS models for sulfate (Figure 12) and sulfite (Figure 13) are shown.

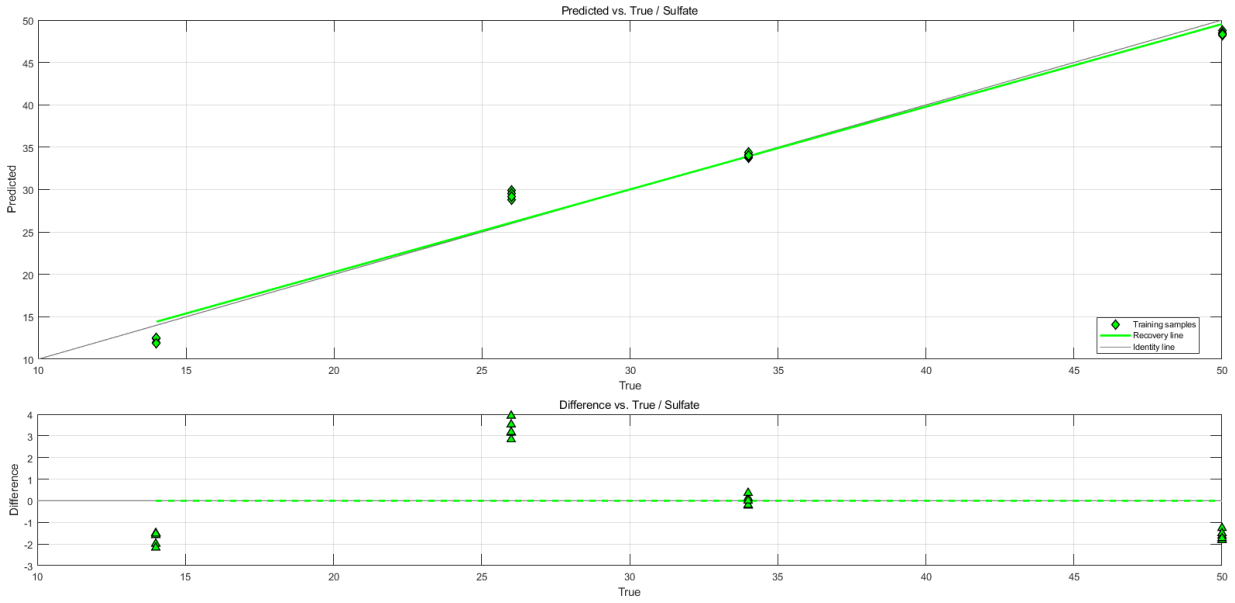

FIGURE 12. PREDICTED VS TRUE AND DIFFERENCE VS TRUE PLOTS FOR SULFATE.

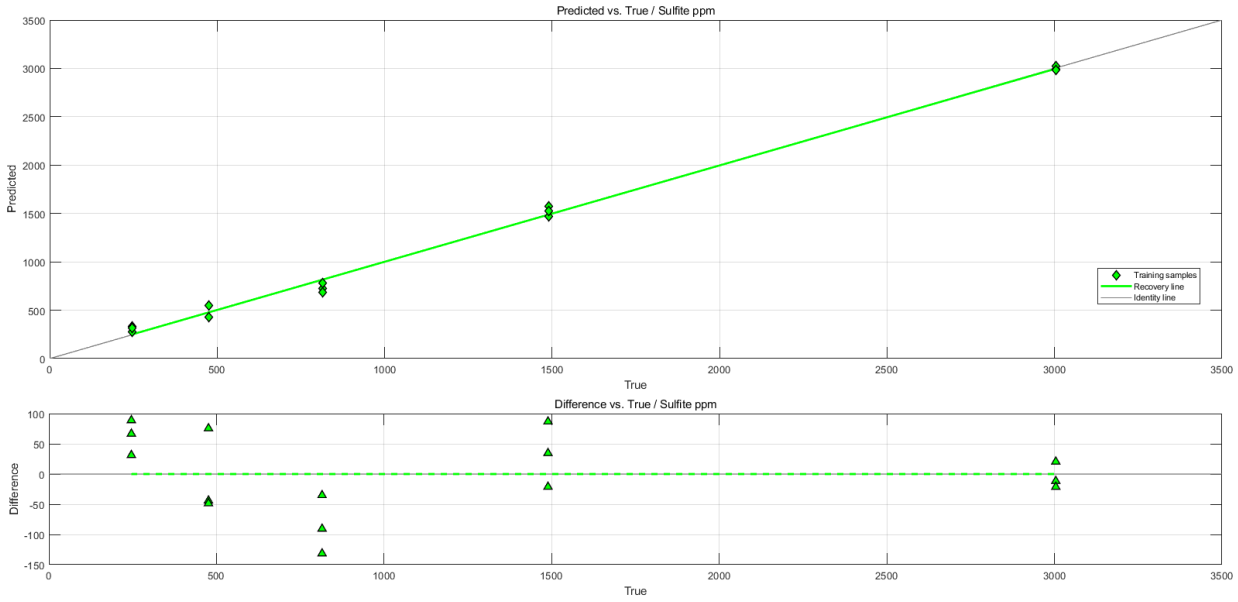

FIGURE 13. PREDICTED VS TRUE AND DIFFERENCE VS TRUE PLOTS FOR SULFITE.

SULFATE AND SULFITE DISCUSSION

In the sulfate samples, the band near 1000cm^{-1} had the strongest response but would not allow it to necessarily be distinguished from the other compounds. However, the bands at 450cm^{-1} and 625cm^{-1} allow for sulfate to be distinguished from the other compounds. The sulfite band has significant overlap with other compounds, however the shape or absence of other bands seen in phosphate and sulfate can allow it to be distinguished from those compounds.

PERCHLORATE RESULTS

Figure 14 shows the spectra of perchlorate. Perchlorate was measured over a range of 0.1ppm to 21ppm.

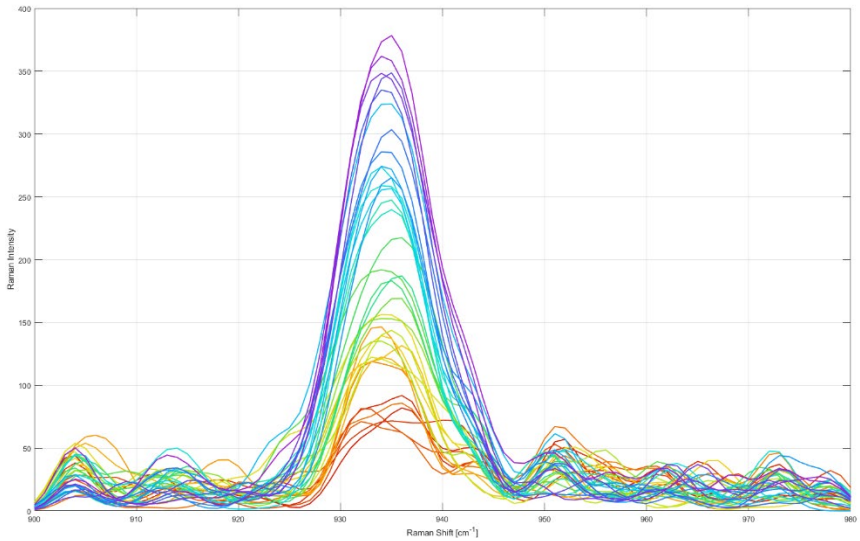

FIGURE 14. SPECTRA FOR PECHLORATE SAMPLES FROM 0.1PPM TO 21PPM.

A one-factor PLS model was made from the perchlorate spectra. The predicted versus true and difference versus true plots corresponding to the PLS model for perchlorate are shown in Figure 15.

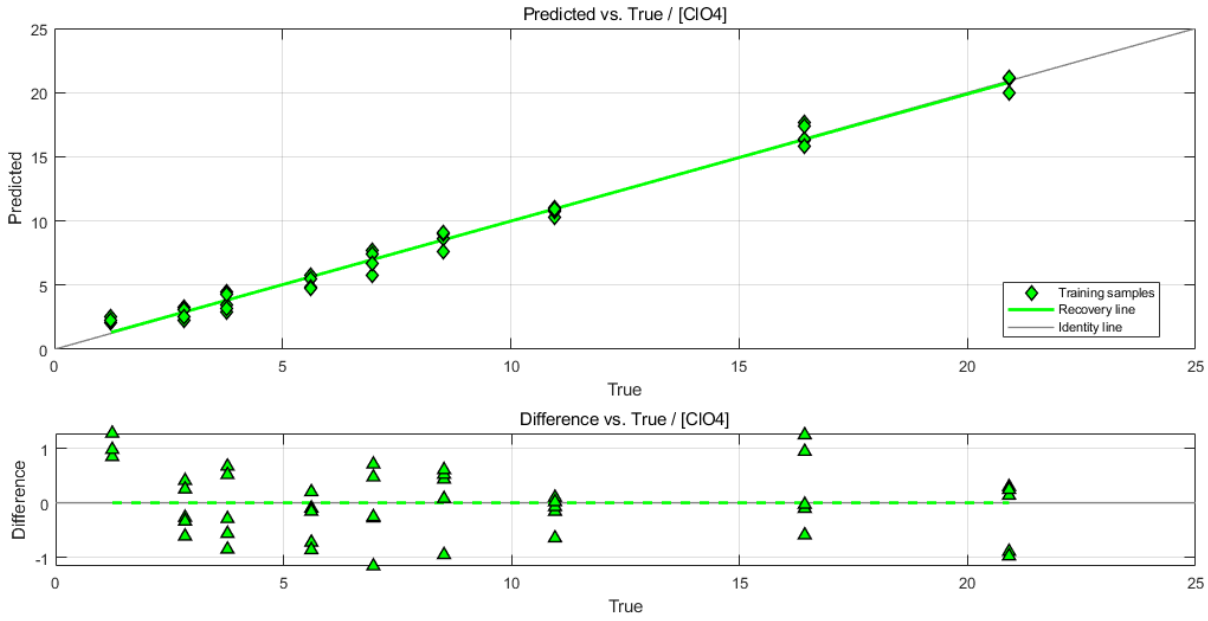

FIGURE 15. PREDICTED VS TRUE AND DIFFERENCE VS TRUE PLOTS FOR PERCHLORATE.

PERCHLORATE DISCUSSION

Perchlorate should be able to be easily detected and quantified due to its strong response. The band associated with perchlorate was distinct from the other compounds. Perchlorate had the lowest limit of detection (<3ppm) among the compounds that were evaluated.

UREA RESULTS

Figure 16 shows the spectra of urea. Urea was measured over a range of 250ppm to 3000ppm.

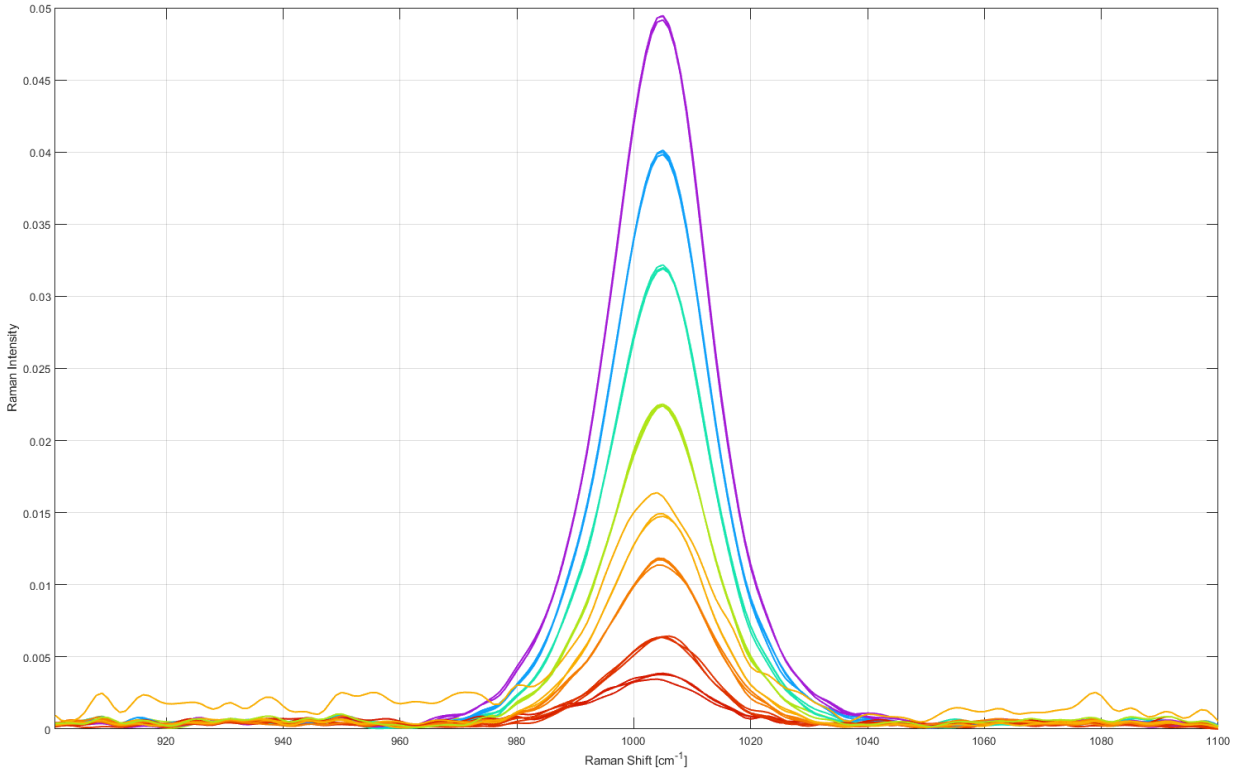

FIGURE 16. SPECTRA FOR UREA FROM 250PPM TO 3000PPM.

A one-factor PLS model was made from the urea spectra. The predicted versus true and difference versus true plots corresponding to the PLS model for urea are shown in Figure 17.

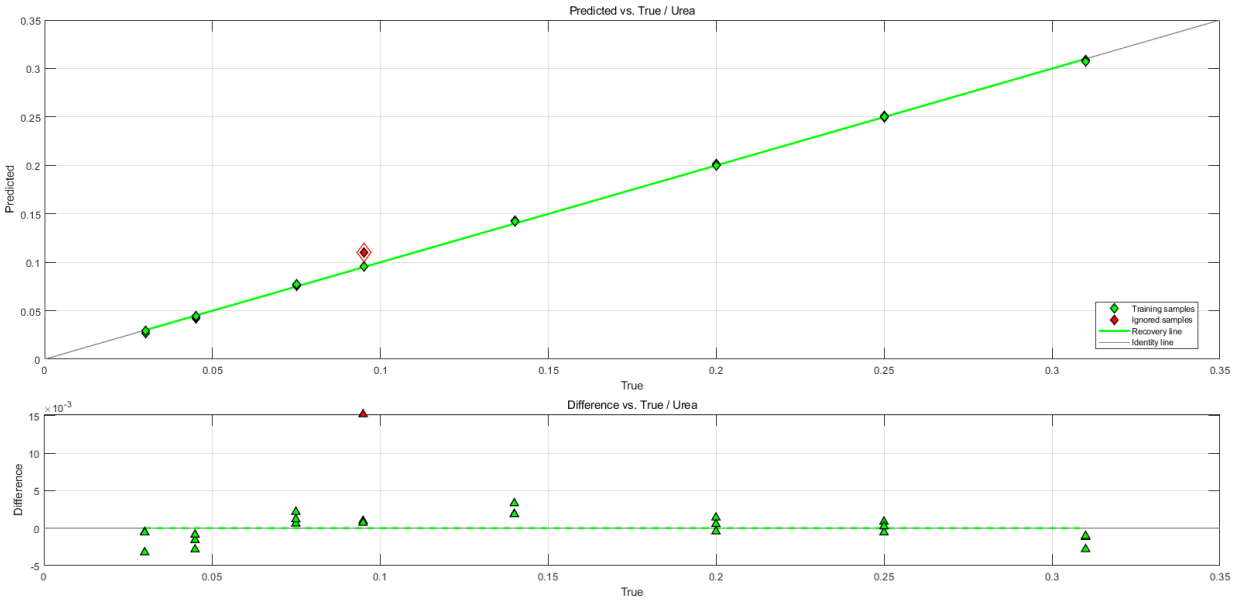

FIGURE 17. PREDICTED VS TRUE AND DIFFERENCE VS TRUE PLOTS FOR UREA.

UREA DISCUSSION

Given its strong response, urea should be able to easily detected and quantified. However, due to the band associated with urea overlapping with the bands of multiple other compounds, this might not always be the case. That said, the width of the urea band may allow for it to be separated from other compounds.

AMMONIUM RESULTS

Figure 18 shows the spectra of ammonium. Ammonium was measured over a range of 0.5% to 5%.

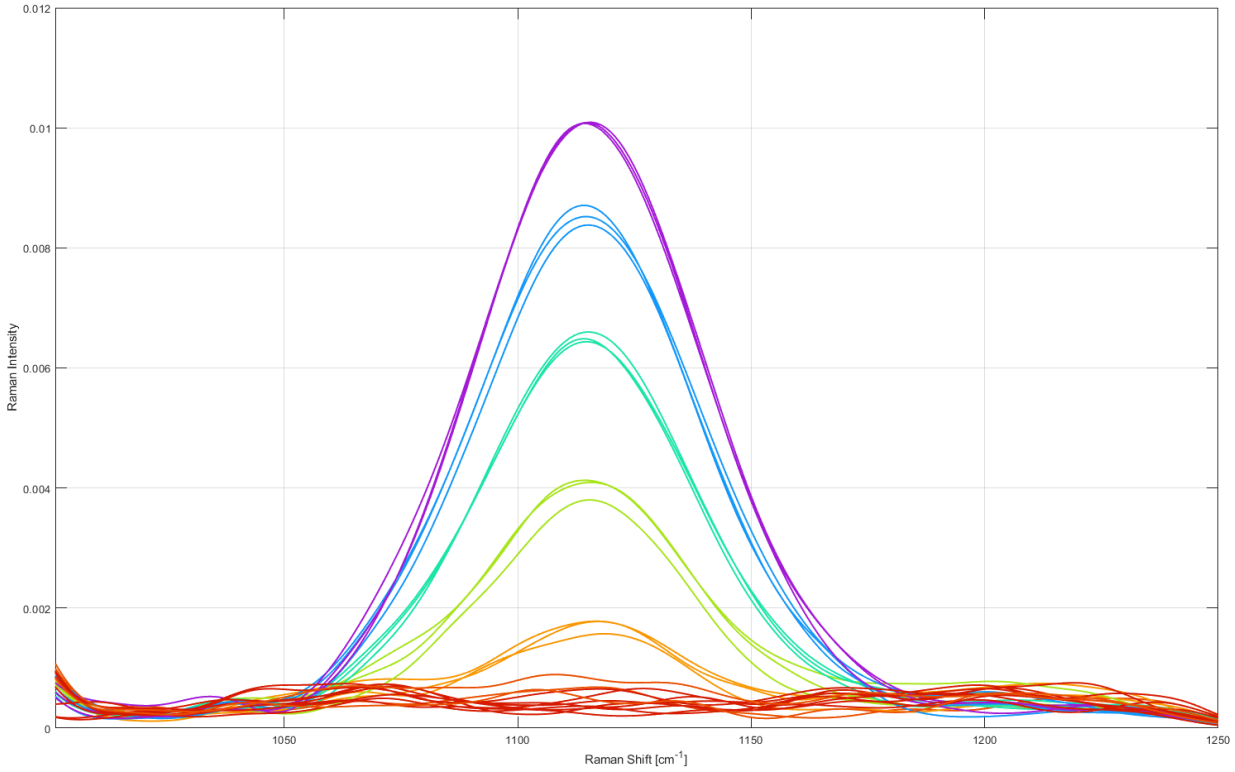

FIGURE 18. SPECTRA FOR AMMONIUM FROM 0.5% TO 5%.

A one-factor PLS model was made from the ammonium spectra. The predicted versus true and difference versus true plots corresponding to the PLS model for ammonium are shown in Figure 19.

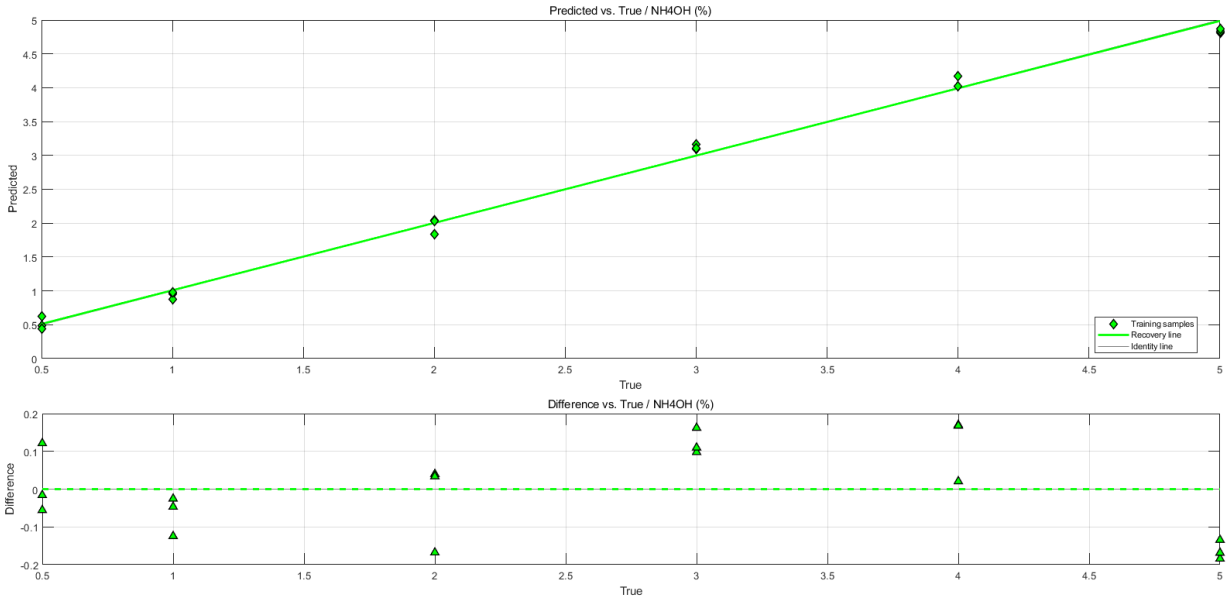

FIGURE 19. PREDICTED VS TRUE AND DIFFERENCE VS TRUE PLOTS FOR AMMONIUM.

AMMONIUM DISCUSSION

The ammonium band shown in Figure 18 is well separated from the bands of the other compounds that were evaluated. However, the response of the ammonium band is weaker than that of many other compounds that were evaluated.

RESIDUAL SOLVENTS RESULTS

Figures 20 and 21 show the spectra of dichloromethane and acetonitrile, respectively. Dichloromethane was measured over a range of 0ppm to 200ppm in water. Acetonitrile was measured over a range of 10ppm to 50ppm.

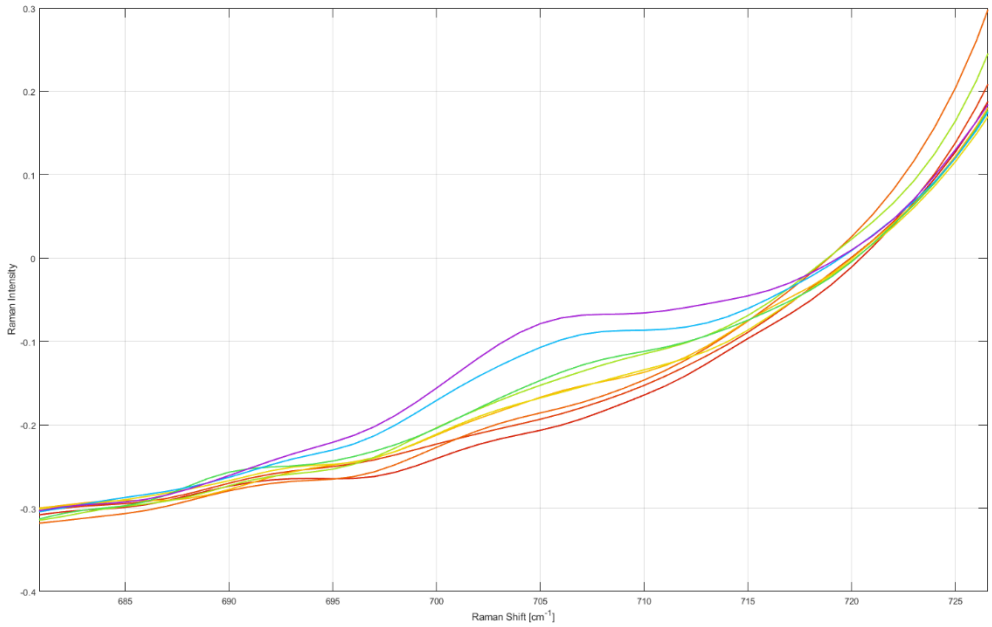

FIGURE 20. SPECTRA OF DICHLOROMETHANE SAMPLES FROM 0PPM TO 200PPM.

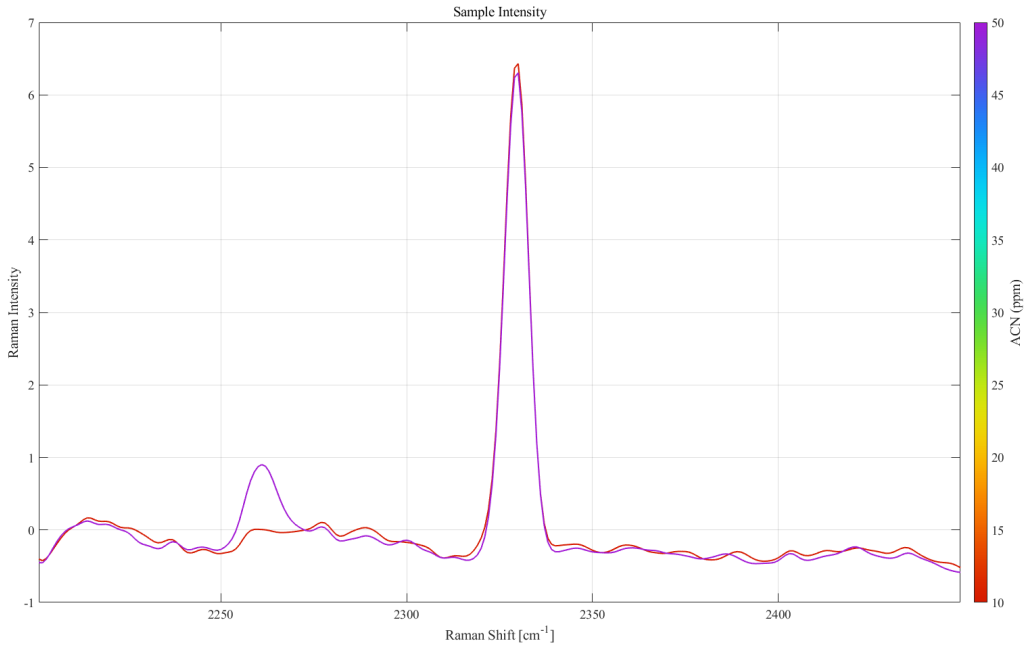

FIGURE 21. SPECTRA OF ACETONITRILE SAMPLES FROM 10PPM TO 50PPM.

A separate PLS model was made for both dichloromethane and acetonitrile. A three-factor PLS model was made from the dichloromethane spectra. A one-factor PLS model was made from the acetonitrile spectra. The predicted versus true and difference versus true plots corresponding to the PLS model for dichloromethane (Figure 22) and acetonitrile (Figure 23, 24) are shown. Figure 23 was made from acetonitrile spectra collected with a mux (multiplexer) and the laser power set to 15mW (as opposed to 495mW).

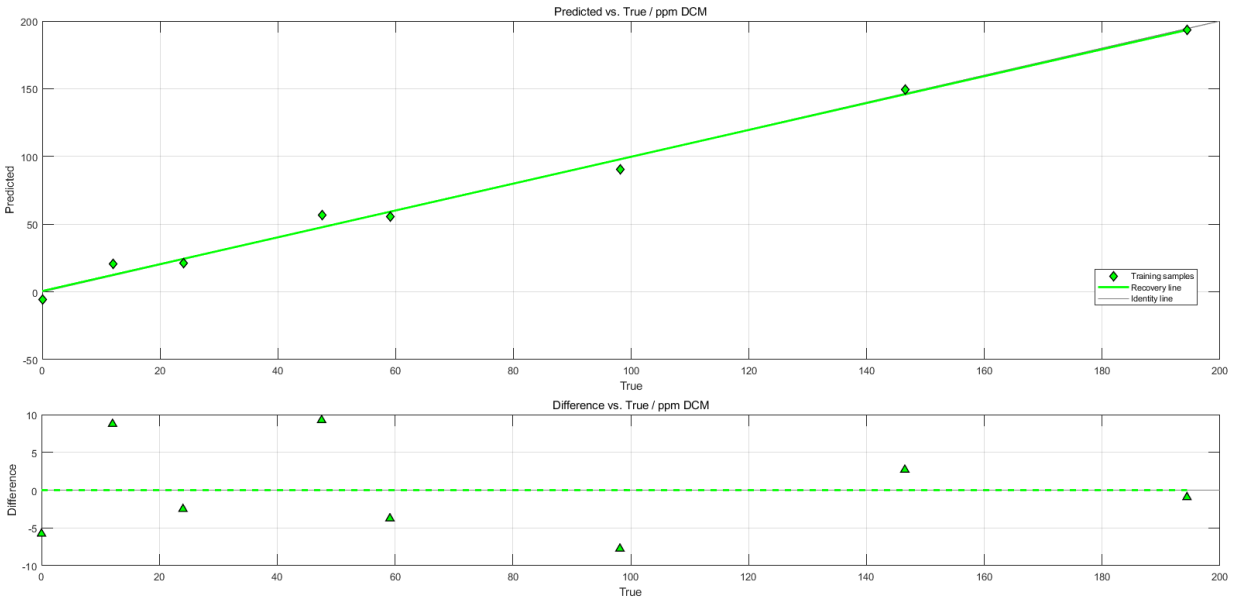

FIGURE 22. PREDICTED VS TRUE AND DIFFERENCE VS TRUE PLOTS FOR DICHLOROMETHANE.

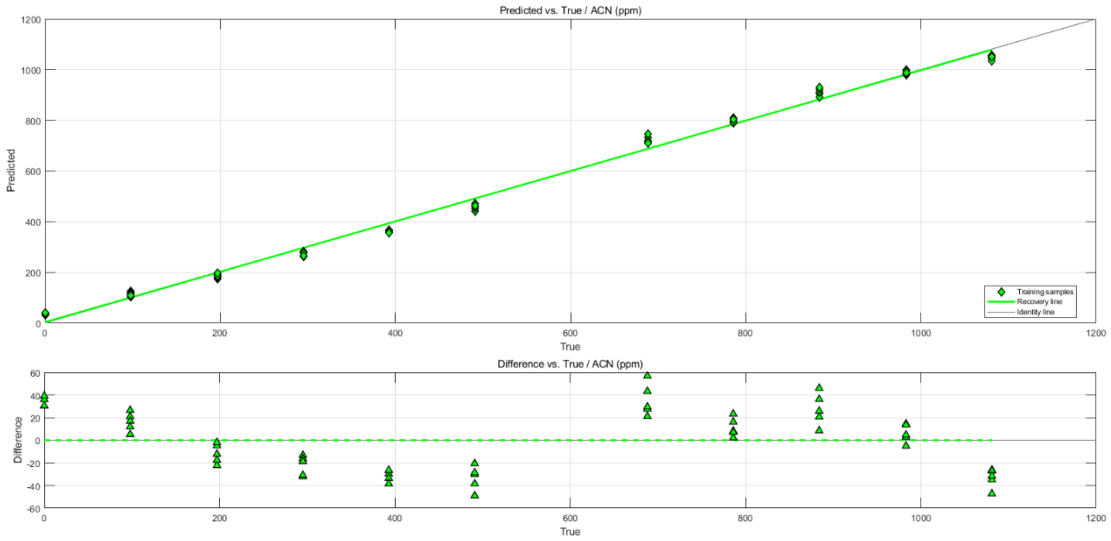

FIGURE 23. PREDICTED VS TRUE AND DIFFERENCE VS TRUE PLOTS FOR ACETONITRILE.

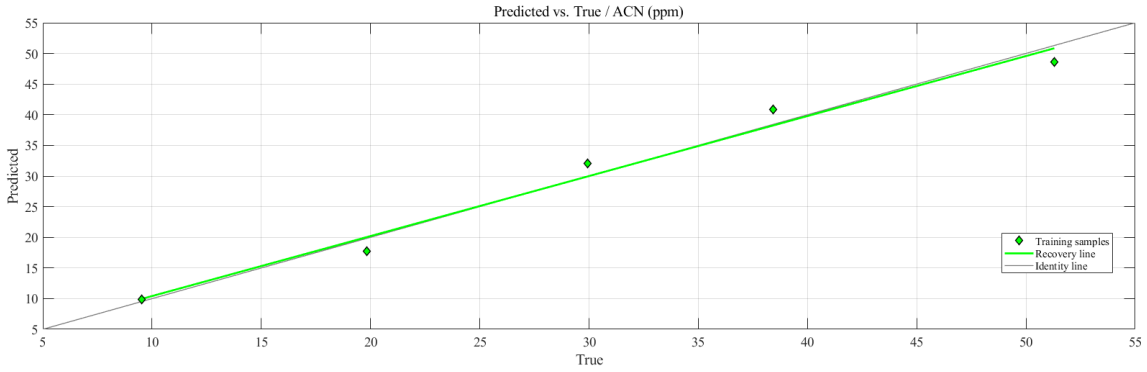

FIGURE 24. PREDICTION VERSUS TRUE PLOT FOR ACETONITRILE.

RESIDUAL SOLVENTS DISCUSSION

Acetonitrile was well separated from the other compounds that were evaluated. Dichloromethane was less well separated but still sufficiently so that it could be easily

distinguished. The laser power of 15mW was used to simulate the intrinsically safe laser setting (OPIS). The multiplexer reduces the signal. This combination is a worst-case scenario in terms of the signal produced. The SuperFlux does not have as high of performance as the HyperFlux but can be used for real-time process measurements.

CONCLUSIONS

A wide variety of compounds that are found in wastewater can be measured with Raman spectroscopy, even with limits of detection as low as 10ppm. Most of these measurements can be performed simultaneously, due to the distinct and well separated bands, and with the same measurement parameters (two-second exposure time, 15 averages, total measurement time of 30 seconds.

ACKNOWLEDGEMENT

The authors would like to acknowledge and thank Colin Couper for collecting the original spectra used in this study.

REFERENCES

Nahiun, Khandakara, Sarker, Bijoyee, Keya, Kamrun, Mahir, Fatin, Shahida, Shahirin, Khan, Ruhul, “A Review on the Methods of Industrial Waste Water Treatment”, Scientific Review, Vol. 7, Issue 3, 20-31.

Metcalf & Eddy, Wastewater Engineering: Treatment and Resource Recovery, 5th ed., McGraw-Hill, New York, NY, 2014.

American Public Health Association, Standard Methods for the Examination of Water and Wastewater, 23rd ed., American Public Health Association, Washington, DC, 2017.

Smith, Ewen and Dent, Geoffrey, Modern Raman Spectroscopy: A Practical Approach, 2nd ed., Wiley, Chichester, UK, 2019.